Preprints of the 19th World Congress
The International Federation of Automatic Control
Cape Town, South Africa. August 24-29, 2014

Residual Capacity Estimation for Ultracapacitors in Electric Vehicles Using Artificial Neural Network

Zhang Lei* Wang Zhenpo Hu Xiaosong*** David. G. Dorrell******

**Beijing Institute of Technology, Beijing, China and University of Technology, Sydney, Australia, (Tel: 61-2-95142921; e-mail: Lei.Zhang-15@ student.uts.edu.au).Corresponding author.*
***Beijing Institute of Technology, Beijing, China, (e-mail: wangzhenpo@bit.edu.cn)*
****Chalmers University of Technology, Gothenburg, Sweden, (e-mail:xiaosong@ chalmers.se)*
*****University of Technology, Sydney, Australia, (e-mail: David.Dorrell@uts.edu.au)*

Abstract: The energy storage system (ESS) plays a significant role in fulfilling the driving performance requirements and ensuring operational safety in an electric vehicle. Ultracapacitors (UCs) are being actively studied and used in parallel with batteries or fuel cells forming hybrid energy storage systems in electric vehicles. They show excellent potential in terms of the sourcing and sinking of power, particularly for the peak-power demand encountered in aggressive regenerative braking. Since there are an increasing number of ultracapacitor applications, which now includes commercial automotive applications, establishing a good model to represent their dynamics, especially the residual capacity estimation (RCE), is vital; but this is challenging. This paper presents a residual capacity estimation model which is based on an artificial neural network (ANN). This takes both charging and discharging current and temperature into consideration. The proposed ANN model comprises of three inputs and one output: the inputs are temperature, current and voltage, and the output is the residual charge. The model is trained and validated by feeding a test database which is extracted from experimental testing of ultracapacitors at different currents and temperatures on a well-established test rig. The training data should span the whole prediction scope, therefore the test currents and temperatures both vary over a wide range and cover all the possible operational conditions of the on-board ultracapacitors. The Back-Propagation (BP) algorithm, together with an early stopping strategy, is adopted to train the proposed ANN model to assure adequately accurate prediction while avoiding overfitting risks. The model performance is validated with experimental results over a set of test data randomly selected.

1. INTRODUCTION

Electric vehicles have been recognized as an important ingredient in a high-efficiency and clean transportation network. The Energy Storage System (ESS) largely affects the performance and cost of an electric vehicle. Ultracapacitors (UCs), also known as supercapacitors or electrochemical double-layer capacitors, are gaining increasing attention for use in an ESS since they are characterized by higher power density, higher energy efficiency and longer cycle life than batteries. UCs also have short charging time and wide operating temperature range. These advantages enable UCs to be a good augmentation to the batteries to constitute a hybrid energy storage system (HESS). The UCs are obliged to offer transient high-power delivery to alleviate battery stress during harsh accelerations and help store regenerative energy in aggressive decelerations.

However, UCs can only store a limited amount of charge, which implies that the state of charge may have an acute and large variation when used. Temperature is also a concerning issue; their performance is highly sensitive to the operational ambient and overheatting may lead to safety hazards. Therefore, it is necessary to establish a model that can represent UC behaviour and estimate the residual capacity precisely under different temperatures. This will lead to the implementation of an efficient control strategy and ensure operational safety.

Ultracapacitors consist of two electrodes and an ion-permeable separator that prevents physical contact between the two electrodes. These are immersed in an electrolyte solution. When applying a small potential to the terminals, energy storage is primarily formed through electrostatic reaction rather than faradaic reaction, as is the case of batteries. The double-layer capacitor structure is at the interface between a solid electrode material surface and a liquid electrolyte. A pseudo-capacitance can be observed which contributes to the total capacitance of the ultracapacitor. UCs are different from conventional capacitors because they exhibit a nonlinear relationship between the terminal voltage and the residual charge. The performance of a specific UC is subject to its porous electrode materials, geometric structure, related electrolyte properties, as well as manufacturing technology. The physical and chemical equations are complicated and sometimes extremely difficult to derive. Some model parameters and variables are inaccessible without special facilities. Thus, it is challenging and even sometimes impractical to build an exact physics-based model from a micro-scale viewpoint.

In order to establish a simple but useful model that captures the dynamic behaviour of an UC well, researchers have

proposed a set of models based on either equivalent electric circuits or artificial neural networks (ANNs). Equivalent electric circuit methods have been widely used to emulate the dynamics of UCs. In 2000, Spyker and Nelms presented a classical equivalent circuit that includes a capacitor, an equivalent series resistance and an equivalent parallel resistance. The associated parameters were derived by measuring the UC response during charge and rest. Buller *et al.* used the electrochemical impedance spectroscopy (EIS) method to investigate the dynamics of UCs in the frequency domain. They measured and recorded the complex impedances of UCs under a wide range of frequency in order to identify an equivalent circuit model. In 2003, Gualous *et al.* also employed the EIS method to establish a second-order equivalent circuit model while introducing a polynomial equation to represent the temperature effects. In 2004, Nelms *et al.* proposed a ladder circuit model, whose parameters were also determined by ac impedance data. In 2007, Lajnef *et al.* presented a 4 RC-branch equivalent circuit model, where the relationship of the open-circuit voltage with respect to temperature and charging frequency was studied. In 2007, Rafik *et al.* presented a 14 Resistance-Inductance-Capacitor equivalent circuit demonstrating how the operating frequency, thermal conditions and voltage influence an UC. In 2009, Brouji *et al.* integrated health status into a comprehensive model using the EIS method. In 2010, Faranda *et al.* presented a new parameter identification procedure in order to calibrate a simple two-branch circuit model. In 2011, Zhang *et al.* proposed a three-branch model that can accurately simulate charge, redistribution, and self-discharge processes. Wu *et al.* gave an on-line dynamic equivalent circuit model, in which the nonlinear relationships between the model parameters and influencing factors, such as environmental temperature and terminal voltage, were explored.

The ANN technique has been extensively used to model complex nonlinear dynamic systems with great success. Its characteristics are such that it does not require the use of specific analytic formulations and physics-based derivations when modelling a nonlinear system. Instead, the system dynamics can be emulated by feeding a measured database into the configured network to train the ANN neurons until either an acceptable precision or the maximum iteration number is reached. Although an ANN is often trained using limited experimental data, it possesses an inherent ability to identify and respond to patterns that are not the same as the ones with which it was trained. A well-trained ANN can be resilient to highly uncertain and even noise-perturbed input data while still generating accurate outputs. Hence the ANN technique has been researched for use in electrical energy storage devices such as batteries. In 2000, Chan *et al*. applied the ANN technique to develop an available-capacity computation model for lead-acid batteries in electric vehicles. In 2002, Shen *et al*. presented an ANN model for lead-acid batteries, based on the battery discharge current and temperature. The ANN model for the battery available-capacity indicator showed good agreement with the experimental results. Again, Shen *et al*. proposed a residual available-capacity indicator model for nickel-metal hydride batteries using ANN technique with defined training patterns. Cheng *et al*. used an evolutionary neural network to estimate a battery state-of-charge. Several studies have investigated the dynamics of various secondary batteries in electric vehicles using the ANN technique; however, few have applied this approach to UCs. In this paper, the ANN method is used to build a UC residual capacity estimation model which considers the impacts of temperature and charging/discharging currents. The voltage, current and temperature are selected as the inputs of the ANN network and the only output is assigned to the residual charge that is a direct indicator of the residual capacity. The back-propagation method is employed to train the ANN model. An early stopping strategy is adopted to prevent overfitting and improve the generalization of the model. In order to prepare the database for ANN training, an UC test rig, capable of charging and discharging the UC, as well as recording the real-time data, is set up. A test procedure is carefully designed and then fully implemented with the purpose of eliminating the effects of charge redistribution and synchronizing the temperature of the test UC with its ambient.

2. BACK-PROPAGATION BASED ANN MODEL FORMULATION

2.1 The ANN technique description

The residual charge of an UC is highly dependent on its temporal state in terms of its temperature and terminal voltage, as well as past experience such as its charging and discharging current. Because of this, it is reasonable to incorporate the effects of current and temperature when developing models for residual capacity estimation. The ANN technique is an effective and powerful tool for function fitting, pattern recognition, nonlinear system estimation and control. A typical ANN network is composed of an input layer, hidden layers and an output layer. The number of hidden layers and their neurons can be case-oriented. Generally speaking, one hidden layer with a considerable number of neurons can make the ANN network powerful enough to investigate any nonlinear system.

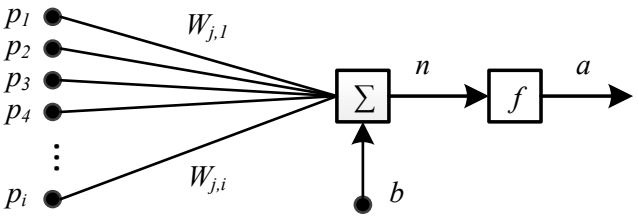

Fig. 1. Schematic depiction of information processing in an ANN neuron

Fig. 1 shows the generic information treatment process through one ANN neuron. In this paper, a multi-input-single-output ANN network is proposed. The three inputs are assigned to temperature, terminal voltage and charging/ discharging current. The only output is the residual charge. The neuron has a bias, which is summed with the weighted

inputs to form the net input. The process function can be expressed as

$$a = f(w_{j,1}p_1 + w_{j,2}p_2 + \ldots + w_{j,i}p_i + b) \quad (1)$$

Where $p_1, p_2, \ldots, p_i$ are the outputs of neurons in the previous layer; $w_{j,1}, w_{j,2}, \ldots, w_{j,i}$ are the weights connecting the j^{th} neuron and all the neurons in the previous layer; b is the bias added to the j^{th} neuron; f is the transfer function of the j^{th} neuron; and a is the output of the j^{th} neuron.

A bound and differentiable logistic sigmoid transfer function is used in all the neurons of the hidden layer. The relationship can be described by

$$f_j(net_j^h) = \frac{1}{1+e^{-net_j}} \quad (2)$$

where net_j^h denotes the sum of weighted input nodes of the j^{th} neuron in the hidden layer. A linear function is usually chosen as the transfer function for the only neuron of the output layer. This is

$$f(net^o) = net^o \quad (3)$$

where net^o is the sum of the weighted input nodes of the neuron in the output layer.

However, the logistic sigmoid function becomes saturated when the absolute value of the net input exceeds 3, which will significantly prolong the training time. Therefore, a pre-processing function is applied to normalize the inputs. The pre-processing function processes each row of the input matrix by mapping each entity value into [-1, +1], and this is obtained from

$$p_{u,v,pre} = \frac{p_{u,v} - p_{u,min}}{p_{u,max} - p_{u,min}} \times 2 + p_{u,min} \quad (4)$$

where $p_{u,v,pre}$ is the entity of the normalized input matrix after pre-processing, $p_{u,v}$ is the entity of the input matrix before pre-processing, $p_{u,min}$ is the minimum of the u row of the input matrix, $p_{u,max}$ is the maximum of the u row of the input matrix.

2.2 Bach-propagation training

ANNs have been widely and successfully applied to many fields, most of which use a feed-forward ANN with the back-propagation (BP) as the training algorithm. By using a BP algorithm, the weights are updated at each epoch in such a way that the error between the output of the ANN network and the forehand obtained target should always be diminished using the derivative information. The error is represented by the mean square error (*mse*), which can expressed as:

$$mse = \frac{1}{N}\sum_{k}^{N}(t_k - o_k) \quad (5)$$

where N denotes the number of patterns, t_k denotes the k^{th} target output and o_k denotes the k^{th} network output.

In the training, the Levenberg-Marquardt algorithm is employed to calculate the update weights at each epoch, which uses a search direction that is a cross between the Gauss-Newton direction and the steepest descent direction. It inherits the speed advantage of the Gauss-Newton algorithm and the stability of the steepest descent method, which makes it more robust than the Gauss-Newton method and converges faster than the steepest descent method. The update rule of the Levenberg-Marquardt algorithm can be shown to be

$$\boldsymbol{w}_{k+1} = \boldsymbol{w}_k - (\boldsymbol{J}_k^T\boldsymbol{J}_k + \mu\boldsymbol{I})^{-1}\boldsymbol{J}_k\boldsymbol{e}_k \quad (6)$$

where $\boldsymbol{w}_{k+1}$ is the weight vector at the k+1th epoch, $\boldsymbol{w}_k$ is the weight vector at the k^{th} epoch, $\boldsymbol{J}_k$ is the Jacobian matrix at the k^{th} epoch, μ is the positive combination coefficient called Marquardt factor, and $\boldsymbol{e}_k$ is the output error vector.

The Jacobian matrix contains the first-order derivatives of total error function with respect to the weights at the k^{th} epoch. It can be calculated from

$$J_k = \begin{pmatrix} \frac{\partial \boldsymbol{e}_1}{\partial \boldsymbol{w}_1} & \frac{\partial \boldsymbol{e}_1}{\partial \boldsymbol{w}_2} & \cdots & \frac{\partial \boldsymbol{e}_1}{\partial \boldsymbol{w}_n} \\ \frac{\partial \boldsymbol{e}_2}{\partial \boldsymbol{w}_1} & \frac{\partial \boldsymbol{e}_2}{\partial \boldsymbol{w}_2} & \cdots & \frac{\partial \boldsymbol{e}_2}{\partial \boldsymbol{w}_n} \\ \cdots & \cdots & \cdots & \cdots \\ \frac{\partial \boldsymbol{e}_m}{\partial \boldsymbol{w}_1} & \frac{\partial \boldsymbol{e}_m}{\partial \boldsymbol{w}_2} & & \frac{\partial \boldsymbol{e}_m}{\partial \boldsymbol{w}_n} \end{pmatrix} \quad (7)$$

where m is the number of neurons in the output layer; here m is 1; n is the number of weights within the network.

2.3 Early stopping strategy

The training error of an ANN model always decreases as the training process proceeds. However, the overfitting problem may emerge as the performance begins to deteriorate even though the training error continues to diminish, especially in the late stages of training. An early stopping strategy is a common countermeasure to avoid the overfitting problem and it is adopted in this paper. In this method, the training database is divided into training, validation and test subsets in accordance to an appropriate ratio. The training process will not terminate when the training error reaches its minimum value. Instead, the training is stopped when the validation error increases for a specified number of iterations, and the weights and bias at the minimum of the validation error is returned. It can be assumed that a period of successive increase in validation error indicates the beginning of the overfitting.

3. EXPERIMENTAL SETUP

In order to obtain a database for training and validation of the ANN ultracapacitor model, experimental tests were carried out on a randomly selected singleton cell of a commercially available ultracapacitor with 3000 F and 2.7 V; this is aimed at the electric vehicle market. The tests included charging and discharging of the ultracapacitor repeatedly at different currents and different temperatures. The experimental setup is shown in Fig. 2. It consists of a Digatron Battery Testing System (BTS-600) and Jufu Thermal Test Chamber, which are responsible for charging and discharging the ultracapacitor and creating the desired constant-temperature environment for tests. The Digatron Battery Testing System

can charge the ultracapacitor at any pre-set current within the range of 0 to 300 A as well as recording the online terminal voltage and charging current. The sample time can be set as small as 10 ms. The temperature that the thermal chamber can provide varies between -40℃ and +60℃. In order to offset the disturbing factors, a test procedure was designed and implemented deliberately in the laboratory. The experimental steps were

- The ultracapacitor was first discharged to a terminal voltage of 0 V, and then short-circuited for 24 hours to eliminate the effect of the charge redistribution within the ultracapacitor.
- The totally-discharged ultracapacitor was then held for 6 hours in the thermal chamber where the temperature was carefully pre-set at certain values to synchronize the temperature of the ultracapacitor and its ambient environment.
- Finally the ultracapacitor was charged at a constant current to the rated voltage while the terminal voltage and current were logged by the computer.

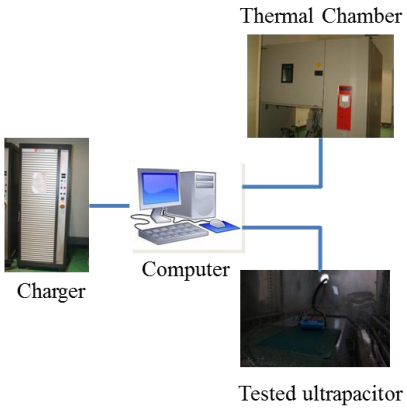

Fig. 2. Experimental Setup

The ultracapacitor was repeatedly charged and discharged using the procedure described above under different circumstances as shown in the Table 1. Three currents: 10A, 25A, and 50A were selected to represent the possible working current levels, and a set of eleven different temperatures from -40℃ to +60 ℃ were used. The voltage evolutions as a function of time during the charging phase under the three currents levels are shown in Figs. 3 to 5; each with the highest, the medium and the lowest temperatures of the selected currents. All three figures show that the charging time becomes greater as the temperature increases. There are several reasons leading to such a difference. The first is that the variation of temperature results in the changes of the parameters within the ultracapacitor. The second is assigned to the capacitance variations with temperature. In fact the capacitance varies with temperature because the properties of activated carbon used in the ultracapacitor, the ionic conductivity of the electrolyte and the effective thickness of the formed double layer capacitor change under different temperatures.

Table 1. Test Scheme

Current (A)	Test Temperature (℃)										
	-40	-30	-20	-10	0	10	20	30	40	50	60
10	T	T	T	T	T	T	T	T	T	T	T
25	T	T	T	T	T	T	T	T	T	T	T
50	T	T	T	T	T	T	T	T	T	T	T

T: test was applied under the column temperature and the row current.

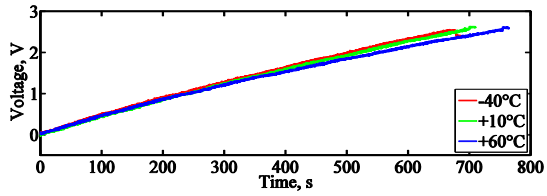

Fig. 3. Ultracapacitor charge curves at the current of 10A under different temperatures

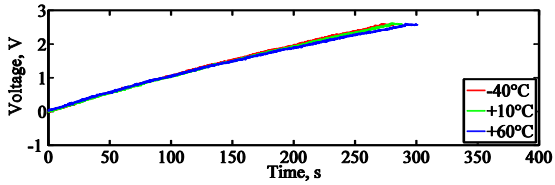

Fig. 4. Ultracapacitor charge curves at the current of 25A under different temperatures

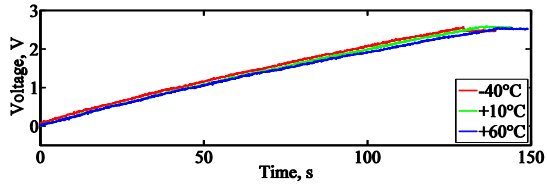

Fig. 5. Ultracapacitor charge curves at the current of 50A under different temperatures

4. OUTCOME AND DISSCUSSION

A database was built using the experimental tests presented previously. An ANN network with one hidden layer and 50 neurons is considered. This configuration was chosen through a search for the best configuration of the network, which showed that the network performed best when its hidden layer hosted 50 neurons. The proposed model is shown in Fig. 6. The inputs of the proposed ANN model are assigned to terminal voltage (V), temperature (T) and charging/ discharging current (I). The only output of the model is the residual charge (q). The training termination condition was set and shown in Table 2.

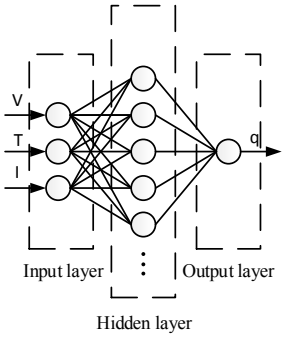

Fig. 6. The configuration of the proposed ANN model for residual charge estimation for ultracapacitors

Table 2. Termination condition

Maximum epoch	Minimum Gradient	Maximum validation increase
1000	10e-5	6

Fig. 7 shows the process of the training. The mean square errors of training, validation and test evolve in similar routes. Their values decrease as the training process proceeds until it terminates at epoch 846, where a 6-epoch successive increase of the validation mean square error is spotted. This means the model is more prone to compromise on the generalization if the training continues. Fig. 8 shows the evolution of the gradient, Marquardt factor and validation checks during the training process, respectively. The third subplot clearly illustrates that the validation check increased by 6 epochs successively when the training terminated.

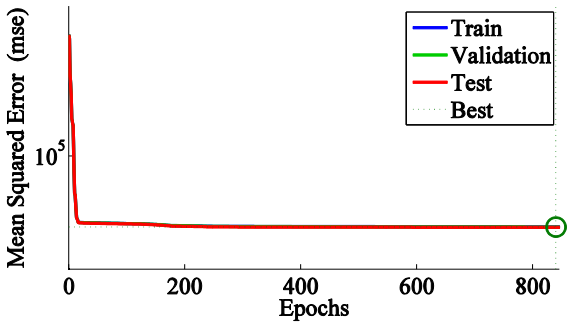

Fig. 7. The mean square error evolution during the training process

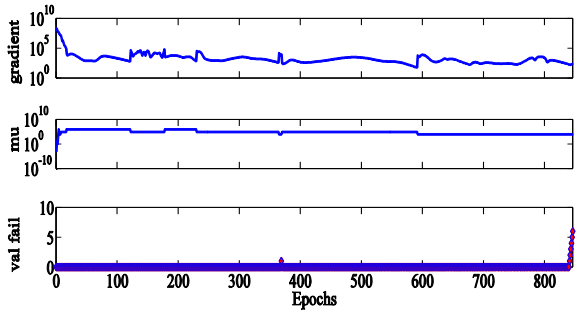

Fig. 8. The evolution of the parameters during the training process

Fig. 9 shows that the regressions of the model outputs and target outputs based on training, validation and test database, are all satisfactory with the regression factors all above 0.999. This means a robust capability of prediction as well as good generalization.

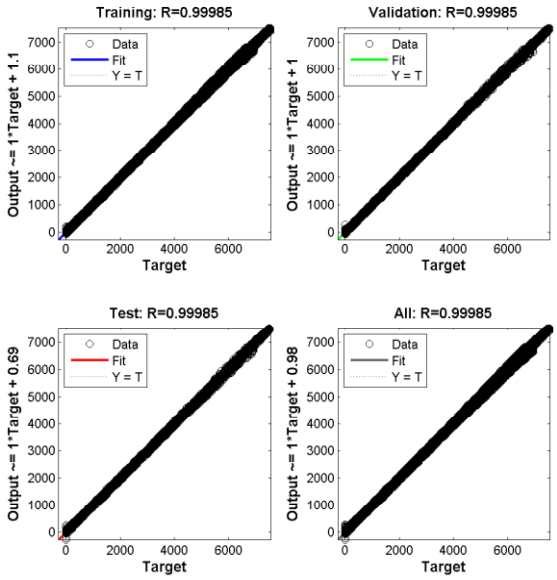

Fig. 9. Regressions of training, validation and test based outputs.

5. CONCLUSION

In this paper, an ANN model is proposed in order to predict the residual capacity of an ultracapacitor as used in electric vehicle applications. The proposed model consists of input layer, output layer and one hidden layer with 50 neurons. Voltage, current and ambient temperature are selected as the inputs of the model, and the only output is assigned to residual charge. A test rig and a well-designed test procedure were set up and used to attain the training database. The back-propagation method, together with pre-processing and an early stopping strategy, is employed to train, validate and test the network. The result shows that the proposed model can provide an accurate prediction of residual charge while maintaining good generalization capability. The established model can be used to precisely monitor the state of charge of the ultracapacitors in ESS, and lays a reliable foundation for control strategy implementation and operation safety.

REFERENCES

Bo, C., B. Zhifeng, and C. Binggang (2008). State of charge estimation based on evolutionary neural network. *Energy Conversion and Management,* **49,** 2788-2794.

Bonert, R. and L. Zubieta (1997). Measurement techniques for the evaluation of double-layer power capacitors. In: *Industry Applications Conference, Conference Record of the 1997 IEEE,* **2,** 1097-1100.

Buller, S., E. Karden, D. Kok, and R. W. De Doncker (2001). Modeling the dynamic behavior of supercapacitors using

impedance spectroscopy. *Thirty-Sixth IAS Annual Meeting. Conference Record of the 2001 IEEE,* **4,** 2500-2504.

Cao, J. and A. Emadi (2012). A New Battery/UltraCapacitor Hybrid Energy Storage System for Electric, Hybrid, and Plug-In Hybrid Electric Vehicles. *Power Electronics, IEEE Transactions on,* **27(1),** 122-132.

Chan, C. C., E. W. C. Lo, and S. Weixiang (2000). The available capacity computation model based on artificial neural network for lead–acid batteries in electric vehicles. *Journal of Power Sources,* **87,** 201-204.

Conway, B.E., V. Birss and J. Wojtowicz (1997). The role and utilization of pseudo-capacitance for energy storage by supercapacitors. *Journal of Power Sources,* **66**, 1–14.

El Brouji, E. H., O. Briat, J. M. Vinassa, N. Bertrand and E. Woirgard (2009). Impact of Calendar Life and Cycling Ageing on Supercapacitor Performance. *Vehicular Technology, IEEE Transactions on,* **58,** 3917-3929.

Faranda, R. (2010). A new parameters identification procedure for simplified double layer capacitor two-branch model. *Electric Power Systems Research,* **80,** 363-371.

Gao, L., R. A. Dougal and S. Liu (2005). Power Enhancement of an Actively Controlled Battery/Ultracapacitor Hybrid. *Power Electronics, IEEE Trans,* **20(1),** 236-243.

Gualous, H., D. Bouquain, A. Berthon and J. M. Kauffmann(2003). Experimental study of supercapacitor serial resistance and capacitance variations with temperature. *Journal of Power Sources,* **123,** 86-93.

Hu, X., S. Li and H. Peng (2012). A comparative study of equivalent circuit models for Li-ion batteries. *Journal of Power Sources,* **198,** 359-367.

Hu, X., Li, S., Peng, H., & Sun, F. (2012). Robustness analysis of State-of-Charge estimation methods for two types of Li-ion batteries. *Journal of Power Sources,* **217,** 209-219.

Sun, F., Hu, X., Zou, Y., & Li, S. (2011). Adaptive unscented Kalman filtering for state of charge estimation of a lithium-ion battery for electric vehicles. *Energy,* **36(5),** 3531-3540.

Kiranyaz, S., T. Ince, A. Yildirim and M. Gabbouj (2009). Evolutionary artificial neural networks by multi-dimensional particle swarm optimization. *Neural Networks,* **22,** 1448-1462.

Lajnef, W., J. M. Vinassa, O. Briat, S. Azzopardi and E. Woirgard (2007). Characterization methods and modelling of ultracapacitors for use as peak power sources. *Journal of Power Sources,* **168,** 553-560.

Lee, D. H., U. S. Kim, C. B. Shin, B. H. Lee, B. W. Kim and Y.-H. Kim (2008). Modelling of the thermal behaviour of an ultracapacitor for a 42-V automotive electrical system, *Journal of Power Sources,* **175,** 664-668.

Nelms, R.M., D. R. Cahela and B. J. Tatarchuk (2003). Modeling double-layer capacitor behavior using ladder circuits. *Aerospace and Electronic Systems, IEEE Transactions on,* **39,** 430-438.

Ortúzar, M., J. Moreno and J. Dixon (2007). Ultracapacitor-Based Auxiliary Energy System for an Electric Vehicle: Implementation and Evaluation. *Power Electronics*, *IEEE Trans,* **54(4),** 2147-2156.

P. Bentley, D. A. Stone and N. Schofield (2005).The parallel combination of a VRLA cell and supercapacitor for use as a hybrid vehicle peak power buffer. *Journal of Power Source,* **147,** 288-294.

Rafik, F., H. Gualous, R. Gallay, A. Crausaz and A. Berthon (2007). Frequency, thermal and voltage supercapacitor characterization and modeling. *Journal of Power Sources,* **165,** 928-934.

Schiffer, J., D. Linzen and D. U. Sauer (2006). Heat generation in double layer capacitors. *Journal of Power Sources,* **160,** 765-772.

Shen, W. X., C. C. Chan, E. W. C. Lo, and K. T. Chau (2002). A new battery available capacity indicator for electric vehicles using neural network. *Energy Conversion and Management,* **43,** 817-826.

Shen, W. X., K. T. Chau, C. C. Chan and E. W. C. Lo (2005). Neural network-based residual capacity indicator for nickel-metal hydride batteries in electric vehicles. *Vehicular Technology, IEEE Transactions on,* **54,** 1705-1712.

Spyker, R. L. and R. M. Nelms (2000). Classical equivalent circuit parameters for a double-layer capacitor. *Aerospace and Electronic Systems, IEEE Transactions on,* **36,** 829-836.

Wu, C. H., Y. H. Hung and C. W. Hong (2012). On-line supercapacitor dynamic models for energy conversion and management. *Energy Conversion and Management,* **53,** 337-345.

Yaghini, M, M. M. Khoshraftar and M. Fallahi (2013). A hybrid algorithm for artificial neural network training. *Engineering Applications of Artificial Intelligence,* **26,** 293-301.

Zhang, Y. and H. Yang (2011). Modeling and characterization of supercapacitors for wireless sensor network applications. *Journal of Power Sources,* **196,** 4128-4135.